

Statics, Dynamics and Manipulations of Bright Matter-Wave Solitons in Optical Lattices

P.G. Kevrekidis¹, D.J. Frantzeskakis², R. Carretero-González³, B.A. Malomed⁴, G. Herring¹ and A.R. Bishop⁵

¹ *Department of Mathematics and Statistics, University of Massachusetts, Amherst MA 01003-4515, USA*

² *Department of Physics, University of Athens, Panepistimiopolis, Zografos, Athens 15784, Greece*

³ *Nonlinear Dynamical Systems Group, Department of Mathematics and Statistics, San Diego State University, San Diego CA, 92182-7720, USA, <http://nlds.sdsu.edu/>*

⁴ *Department of Interdisciplinary Studies, Faculty of Engineering, Tel Aviv University, Tel Aviv 69978, Israel*

⁵ *Center for Nonlinear Studies and Theoretical Division, Los Alamos National Laboratory, Los Alamos, NM 87545, USA*

(Dated: In Press Phys. Rev. A, 2005)

Motivated by recent experimental achievement in the work with Bose-Einstein condensates (BECs), we consider bright matter-wave solitons, in the presence of a parabolic magnetic trap and a spatially periodic optical lattice (OL), in the attractive BEC. We examine pinned states of the soliton and their stability by means of perturbation theory. The analytical predictions are found to be in good agreement with numerical simulations. We then explore possibilities to use a time-modulated OL as a means of stopping and trapping a moving soliton, and of transferring an initially stationary soliton to a prescribed position by a moving OL. We also study the emission of radiation from the soliton moving across the combined magnetic trap and OL. We find that the soliton moves freely (without radiation) across a weak lattice, but suffers strong loss for stronger OLs.

I. INTRODUCTION

The recent progress in experimental and theoretical studies of Bose-Einstein condensates (BECs) [1] has led to an increase of interest in matter-wave (MW) solitons. One-dimensional (1D) dark [2] and bright [3] solitons have been observed in experiments with repulsive and attractive BECs, respectively. Very recently, bright solitons of the gap type, predicted in repulsive condensates [4], have been created in the experiment [5]. Theoretical predictions concerning a possibility of the existence of stable multi-dimensional solitons supported by a full [4, 6] or low-dimensional [7] optical lattice (OL) have also been reported. The OL is created as a standing-wave interference pattern between mutually coherent laser beams [8, 9, 10, 11, 12, 13].

The study of the MW solitons, apart from being a fundamentally interesting topic, may have important applications. In particular, a soliton may be transferred and manipulated similarly to what has been recently demonstrated, experimentally and theoretically, for BECs in magnetic waveguides [14] and atom chips [15]. More generally, the similarity between bosonic MWs and light waves suggests that numerous results known for optical solitons [16], along with the possibility of manipulation of atomic states (by means of resonant electromagnetic waves governing transitions between different states), may have impact on the rapidly evolving field of quantum atom optics (see, e.g., Ref. [17]).

A context where the dynamics of MW solitons is particularly interesting is that of BECs trapped in a periodic potential induced by the above-mentioned OLs. The possibility to control the OL has led to the realization of many interesting phenomena, including Bloch oscillations [10, 18], Landau-Zener tunneling [8] (in the presence of an additional linear external potential), and classical

[19] and quantum [13] superfluid-insulator transitions. A large amount of theoretical work has been already done for nonlinear MWs trapped in OLs (see Refs. [20, 21] for recent reviews).

The objective of this work is to systematically study the statics and dynamics of one-dimensional (1D) bright MW solitons confined in the combination of the parabolic magnetic trap (MT) and OL. Additionally, we examine the possibility to control the motion of the soliton by means of a *time-dependent* OL potential (the latter is available for the experiment). In particular, we will show that, in the case when the OL period is comparable to the characteristic spatial width of the soliton, it is possible to: (a) snare and immobilize an originally moving soliton in a local potential well, by adiabatically switching the OL on, and (b) grasp and drag an initially stationary soliton by a slowly moving OL, delivering it to a desired location. Note that bright MW solitons may travel long distances in the real experiment, up to several millimeters [3], and are truly robust objects, being themselves coherent condensates. Thus, the manipulation of bright MW solitons is a very relevant issue for the physics of BECs.

The paper is organized as follows. In Sec. II, we introduce the model and present analytical results. In Sec. III, we numerically investigate static and dynamical properties of the solitons, and study possibilities to manipulate them as outlined above. The results of the work are summarized in Sec. IV.

II. THE MODEL AND ITS ANALYTICAL CONSIDERATION

The Gross-Pitaevskii equation (GPE), which governs the evolution of the single-atom wave function in the

mean-field approximation, takes its fundamental form in the 3D case. A number of works analyze its reduction to an effective 1D equation in the case of strongly elongated cigar-shaped BECs [22, 23, 24]. In particular, the derivation in Ref. [23] assumed that the potential energy is much larger than the transverse kinetic energy. A general conclusion is that the effective equation reduces to the straightforward 1D version of the GPE. In the normalized form, it reads [20]

$$iu_t = -\frac{1}{2}u_{xx} + g|u|^2u + V(x)u, \quad (1)$$

where $u(x, t)$ is the 1D mean-field wave function (although a different version of the 1D GPE, with a non-polynomial nonlinearity, is known too [24]). The combination of the MT and OL potential corresponds to

$$V(x) = \frac{1}{2}\Omega^2x^2 + V_0\sin^2(kx). \quad (2)$$

In Eq. (1), x is measured in units of the fluid healing length $\xi = \hbar/\sqrt{n_0g_{1D}m}$, where n_0 is the peak density and $g_{1D} \equiv g_{3D}/(2\pi l_\perp^2)$ is the effective 1D interaction strength, obtained upon integrating the 3D interaction strength $g_{3D} = 4\pi\hbar^2a/m$ in the transverse directions (a is the scattering length, m the atomic mass, and $l_\perp = \sqrt{\hbar/m\omega_\perp}$ is the transverse harmonic oscillator length, with ω_\perp being the transverse-confinement frequency). Additionally, t is measured in units of ξ/c (where $c = \sqrt{n_0g_{1D}/m}$ is the Bogoliubov speed of sound), the atomic density is rescaled by the peak density n_0 , and energy is measured in units of the chemical potential of the system $\mu = g_{1D}n_0$. Accordingly, the dimensionless parameter $\Omega \equiv \hbar\omega_x/g_{1D}n_0$ (ω_x is the confining frequency in the axial direction) determines the magnetic trap strength, V_0 is the OL strength, while k is the wavenumber of the OL; the latter, can be controlled by varying the angle θ between the counter-propagating laser beams, so that $\lambda \equiv 2\pi/k = (\lambda_{\text{laser}}/2)\sin(\theta/2)$ [25]. Finally, $g = \pm 1$ is the renormalized nonlinear coefficient, which is positive (negative) for a repulsive (attractive) condensate. As we are interested in the ordinary bright MW solitons, which exist in case of attraction, we will fix $g = -1$.

Without the external potential ($\Omega = V_0 = 0$), Eq. (1) supports bright soliton solutions of the form

$$u_s(x - x_0) = \eta \operatorname{sech}[\eta(x - x_0)] \exp\left(\frac{1}{2}i\eta^2t\right), \quad (3)$$

where η is the soliton's amplitude, and x_0 is the coordinate of its center. Moving solitons can be generated from the zero-velocity one by a Galilean boost.

In the presence of the external potential, the first issue is to identify stationary positions for the soliton. This issue can be addressed, using an effective potential for the soliton's central coordinate (see, e.g., Refs. [26] and [27]), which is defined by the integral

$$V_{\text{eff}}(x_0) = \int_{-\infty}^{+\infty} V(x)|u_s(x - x_0)|^2 dx. \quad (4)$$

Stationary positions of the soliton correspond to local extrema of the effective potential (4). This well-known heuristic result can be rigorously substantiated by means of the Lyapunov-Schmidt theory applied to the underlying nonlinear Schrödinger equation [28]. The effective potential corresponding to the external potential (2), acting on the stationary soliton (3), can be easily evaluated:

$$V_{\text{eff}}(x_0) = \eta\Omega^2x_0^2 - \pi V_0k \cos(2kx_0) \operatorname{csch}\left(\frac{k\pi}{\eta}\right). \quad (5)$$

Notice that, depending on values of the parameters, this potential may have a single extremum at $x_0 = 0$, or multiple ones.

The stability of the soliton resting at a stationary position can also be analyzed in terms of the effective potential (4): the position is stable if it corresponds to a potential minimum. This well-known result can be rigorously derived using the theory of Ref. [29] and reformulated in Ref. [30] (see also Refs. [31] and [32]). In particular, the curvature of the potential at the stationary position determines the key linearization eigenvalue λ , that may cause an instability, bifurcating through the origin of the corresponding spectral plane (this feature is revealed by the heuristic [26] and rigorous [30] analysis). The eigenvalue is easily found to be

$$\lambda^2 = -\eta^{-1/2}V_{\text{eff}}''(x_0), \quad (6)$$

confirming that minima and maxima of the effective potential (4) give rise, respectively, to stable ($\lambda^2 < 0$) and unstable ($\lambda^2 > 0$) equilibria.

We note in passing (this will be important in what follows) that the minima of the effective potential (4) *differ* from the minima of the external potential $V(x)$ trapping the atoms. For instance, for $\eta = \sqrt{2}$, $V_0 = 0.25$ and $\Omega = 0.1$, the first three minima of $V(x)$ (apart from the one at $x = 0$) are located at the points $x = 3.0789, 6.1587, 9.2356$, while the minima of V_{eff} are found at $x_0 = 3.0166, 6.0247, 9.0089$.

We now turn to numerical results, aiming to examine the validity of the theoretical predictions, as well as to perform dynamical experiments using the OL to guide the soliton motion.

III. NUMERICAL RESULTS

A. Stability of the solitons

We begin the numerical part by examining the steady-state soliton solutions and their stability in the context of Eq. (1). Such solutions are sought for in the form $u(x, t) = \exp(i\Lambda t)w(x)$, which results in the stationary equation,

$$\Lambda w = (1/2)w_{xx} + w^3 - V(x)w. \quad (7)$$

To examine the linear stability of the solitons, we take a perturbed solution as

$$u(x) = e^{i\Lambda t} \left[w + \epsilon \left(a(x)e^{-i\omega t} + b(x)e^{i\omega^* t} \right) \right], \quad (8)$$

where ϵ and ω are an infinitesimal amplitude and (generally speaking, complex) eigenfrequency of the perturbation, and linearize Eq. (1).

Equations (1) and (2), with $g = -1$ and arbitrary coefficients V_0, Ω and k , possess a scaling invariance, which allows us to fix $\Lambda = 1$ (hence $\eta = \sqrt{2}$). It should be noted that, in the absence of the MT ($\Omega = 0$), the soliton's frequency should be chosen so that it belongs to a bandgap in the spectrum of the linearized Eq. (1) with the periodic potential (2), to avoid resonance with linear Bloch waves. However, the MT potential with finite Ω makes this condition irrelevant. In principle, it might be interesting to investigate how the increase of Ω from zero gradually lifts the condition of the resonance avoidance, but this more formal issue is left beyond the scope of the present work.

To estimate actual physical quantities corresponding to the above normalized values of the parameters, we consider a cigar-shaped ${}^7\text{Li}$ condensate containing $N \simeq 10^3$ atoms in a trap with $\omega_x = 2\pi \times 25$ Hz and $\omega_\perp = 70\omega_x$. Then, for a 1D peak density $n_0 = 10^8$ m $^{-1}$, the parameter Ω in Eq. (2) assumes the value $\Omega = 0.1$, while the time and space units correspond to 0.3 ms and 1.64 μm , respectively. These units remain valid for other values of Ω , as one may vary ω_\perp and change ω_x accordingly; in this case, other quantities, such as N , also change.

Figure 1 summarizes our numerical findings for the stability problem. As expected, the (*zeroth-well*) solution for the soliton pinned at $x_0 = 0$ exists and it is stable for all values of the potential's parameters. We have typically chosen to fix $\Omega = 0.1$ and $k = 1$ (i.e., $\lambda = 2\pi$) and vary V_0 ; however, it has been checked that the results presented below adequately represent the phenomenology for other values of (Ω, k) as well.

The next (*first-well*) solution, corresponding to the potential minimum closest to $x_0 = 0$, exists for values of the MT strength V_0 smaller than a critical one $V_0^{(\text{cr})}$. Within the accuracy of 0.0025, we have found its numerical value to be $V_0^{(\text{cr})}|_{\text{num}} = 0.045$, in very good agreement with the prediction following from the analytical approximation (5) for the effective potential, which shows that the corresponding potential minimum disappears, merging with a maximum, at $V_0^{(\text{cr})}|_{\text{anal}} \approx 0.048$. The corresponding pinned-soliton solution is indeed stable prior to its disappearance, in agreement with the analytical prediction based on Eq. (6).

Similarly, the subsequent (*second-well*) solution, associated with the next potential minimum (if it exists), is found to disappear (for the same parameters) at $V_0^{(\text{cr})}|_{\text{num}} = 0.1 \pm 0.0025$, while the analytical approximation (5) yields $V_0^{(\text{cr})}|_{\text{anal}} \approx 0.112$. Finally, a similar result was obtained for the third-well solution: $V_0^{(\text{cr})}|_{\text{num}} = 0.1425 \pm 0.0025$, and $V_0^{(\text{cr})}|_{\text{anal}} \approx 0.176$.

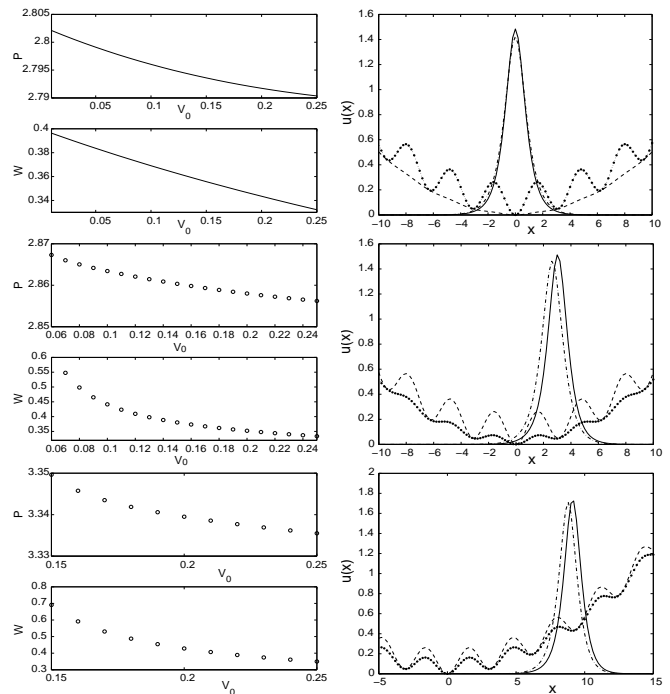


FIG. 1: For each of the three sets of the pictures, the left panel shows the continuation of the soliton branch to values near $V_0^{(\text{cr})}$, at which it disappears (for soliton solutions trapped at different wells). The right panel shows the solution at the initial and final points of the continuation (and the corresponding potentials). The left panels show the norm of the soliton solution (proportional to the number of atoms in the condensate), $P = \int_{-\infty}^{+\infty} |u(x)|^2 dx$, and its squared width, $W = P^{-1} \int_{-\infty}^{+\infty} x^2 |u(x)|^2 dx$, as a function of the OL strength V_0 . The top set of the panels pertains to the zeroth-well solution (the soliton pinned in the central potential well); the solution in the right panel is shown by the solid line for $V_0 = 0.25$, and by the dash-dotted line for $V_0 = 0$. The corresponding potential is shown by the dotted line for $V_0 = 0.25$, and by the dashed line for $V_0 = 0$. Similarly, in the middle set, the solid line (and the dashed one for the potential) correspond to $V_0 = 0.25$, and the dashed-dotted line, together with the dotted one for the potential, correspond to $V_0 = 0.06$ for the first-well solution [notice that this branch terminates at $V_0 \approx 0.045$]. Finally, in the bottom set of the panels, the solid line (and the dashed one for the potential) again correspond to $V_0 = 0.25$, while the dashed-dotted line (and the dotted one for the potential) correspond to $V_0 = 0.15$ for the third-well solution [this branch terminates at $V_0 \approx 0.1425$].

It is quite natural that the discrepancy between the theoretical and the numerical results increases for the higher-well solutions, given that the numerically exact profile of the pinned soliton gets more distorted under the action of the MT. Notice, for example, the difference in the amplitude between the soliton in the top panel and in the one in the bottom panel in Fig. 1, which clearly illustrates this effect.

B. Soliton dynamics and manipulations

Having addressed the existence and stability of the solitons, we now proceed to study their possible dynamical manipulation by means of the OL. First, we examine the possibility to trap a soliton using the secondary minima in the OL potential. In particular, it is well known that, in the absence of the OL, the soliton in the magnetic trap, when displaced from the center, $x_0 = 0$, executes harmonic oscillations with the frequency Ω , as a consequence of the Ehrenfest theorem (alias the Kohn's theorem [33], which states that the motion of the center of mass of a cloud of particles trapped in a parabolic potential decouples from the internal excitations). This result can also be obtained using the variational approximation [34] and, more generally, is one of the results obtained from the moment equations for the condensate in the parabolic potential [35].

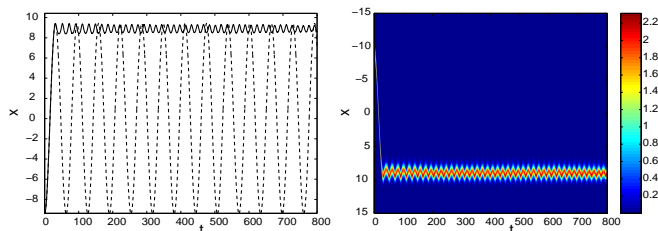


FIG. 2: (color online) An example of snaring the originally moving soliton using the optical lattice. The left panel shows the motion of the soliton's center of mass. The dashed line shows the situation without the OL (but in the presence of the magnetic trap). If we turn on the OL potential, as the soliton arrives at the turning point of its trajectory, it gets captured by the secondary minimum of the full potential, created in a vicinity of this point. The right panel shows the same, but through the space-time contour plots of the local density, $|u(x,t)|^2$.

A new issue is whether one can capture the soliton performing such oscillations by turning on the OL. Focusing, as previously, on the most relevant case when the width of the soliton is comparable to the OL wavelength, we display an example of the capture in Fig. 2. The dashed and solid lines show, respectively, the harmonic oscillations in the absence of the OL, and a numerical experiment, where, at the moment when the soliton arrives at the turning point (it is $x = 3\pi$ for this case, i.e., the third potential minimum), we abruptly turn on the OL, so that

$$V(x,t) = \frac{1}{2}\Omega^2 x^2 + \frac{1}{2}V_0 \left[1 + \tanh\left(\frac{t-t_0}{\tau}\right) \right] \sin^2(kx). \quad (9)$$

Here t_0 and τ are constants controlling, respectively, the switch-on time and duration of the process; in the simulations, we use $t_0 = 31.7$ and $\tau = 0.1$. We clearly observe that, contrary to the large-amplitude oscillations of the soliton taking place when the OL is absent, the soliton is

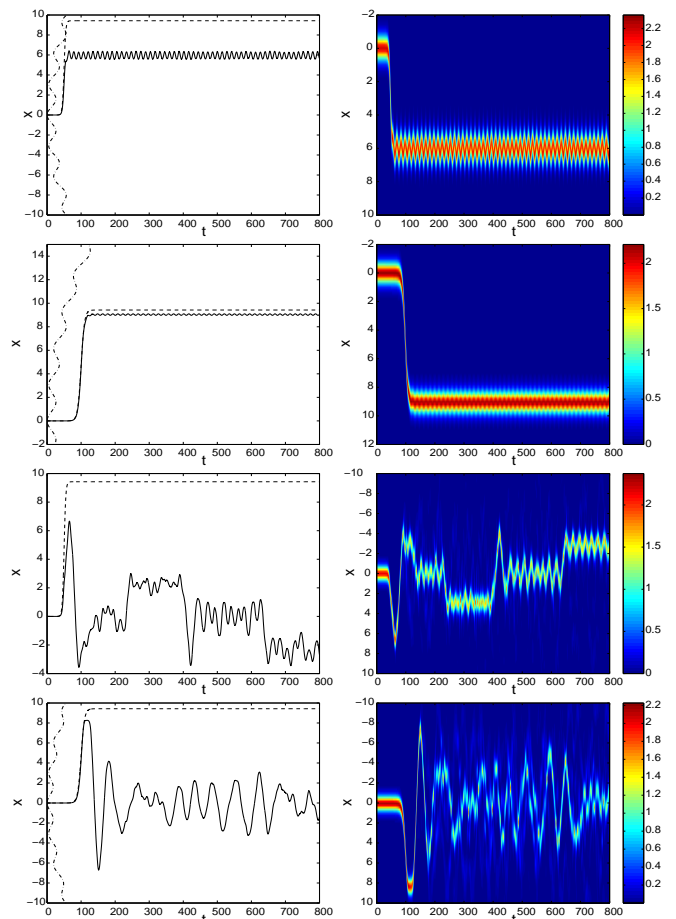


FIG. 3: (color online) Panels have the same meaning as in Fig. 2, but now for the case of a moving OL. The left panel shows the soliton's center of mass by the solid line and the potential of the OL's center by the dashed line. The potential $V(x,t=0)$ is sketched by the dash-dotted line to illustrate the structure and location of the potential wells. The right panel again shows the space-time contour plot of $|u(x,t)|^2$. The top set of the panels is generated with $t_0 = 50$ and $\tau = 5$ in Eq. (9). The second set pertains to $t_0 = 100$ and $\tau = 10$ (both have $V_0 = 0.25$). The situation for a shallower well, with $V_0 = 0.17$, is shown in the third and fourth panels. In all cases, $x_{\text{ini}} = 0$ and $x_{\text{fin}} = 3\pi$.

now fully captured (for very long times) by the potential minimum newly generated by the optical trap.

Instead of being a means to snare for moving soliton, the OL may also be used as a means of moving the soliton in a prescribed way, i.e., as a “robotic arm” depositing the soliton at a desired location (see, e.g., [36]). This possibility is demonstrated (with varying levels of success) in Fig. 3. The top two sets of figures are performed for a strong OL ($V_0 = 0.25$), while the bottom two are used for a weaker OL potential (with $V_0 = 0.17$). In all the cases the potential used is

$$V(x) = \frac{1}{2}\Omega^2 x^2 + V_0 \sin^2(k(x - y(t))), \quad (10)$$

where the position of the OL is translated according to

$$y(t) = x_{\text{ini}} + \frac{1}{2}(x_{\text{fin}} - x_{\text{ini}}) \left[1 + \tanh\left(\frac{t - t_0}{\tau}\right) \right]. \quad (11)$$

Here x_{ini} and x_{fin} are, respectively, the initial and final (target) positions of the soliton. In the case under consideration, $x_{\text{ini}} = 0$ and $x_{\text{fin}} = 3\pi$, i.e., the aim is to transport the MW soliton from the central well to the third one, on the right of the center. In the top set of the panels with $t_0 = 50$ and $\tau = 5$, we observe what happens if the motion of the potential center is not sufficiently slow to adiabatically transport the soliton to its final position. In particular, the soliton gets trapped in the second well, without being able to reach its destination. However, we observe that this difficulty can be overcome, if the transport is applied with a sufficient degree of adiabaticity; see, e.g., the middle panel with $t_0 = 100$ and $\tau = 10$, which succeeds in delivering the soliton at the desired position. Notice that the final position of the center of the OL is at $y = 3\pi$, which is different from the center of the third well of the effective potential, around which the soliton will oscillate, upon arrival. The theoretical prediction that was presented above (for $V_0 = 0.25$) for this well is $x_0 = 9.0089$, while in the simulations the soliton oscillates around 9.04 in very good agreement with the theory. The two lower sets of the panels are meant to illustrate that adiabaticity is not the single condition guaranteeing the efficient transport. The numerical experiments are performed for a shallower potential where the relevant well (to which the soliton is to be delivered) is near the threshold of its existence. As a result, neither in the case with $\tau = 5$ (the third set of panels), nor in the one with $\tau = 10$, is the OL successful in transporting the soliton at the desired position.

A similar numerical experiment in the absence of the magnetic trap is shown in Fig. 4. The top panels display the successful transfer of the soliton by the OL of a form similar to that in Eq. (9), with $\Omega = 0$ and $V_0 = 0.25$, for $t_0 = 100$ and $\tau = 10$. Notice that, in the present case, the final positions of the OL's center and of the soliton coincide [as the atomic potential and the effective potential for the soliton have the same set of minima in this case, cf. Eq. (5)]. However, once again, the same experiment, if not performed with a sufficient degree of adiabaticity (as in the bottom panel of Fig. 4, with $t_0 = 50$ and $\tau = 5$), is not successful in depositing the soliton at the prescribed location. Instead, in this case the soliton continues to move along the OL, emitting radiation waves and decreasing its amplitude.

To better illustrate the emission of radiation and its dependence on the depth of the OL (since it is known that the emission is absent in the parabolic potential without the OL ingredient), we have also performed the following numerical experiment. We took the potential of the form

$$V(x) = \frac{1}{2}\Omega^2 x^2 + V_0 \sin^2(kx) + \alpha(t)x, \quad (12)$$

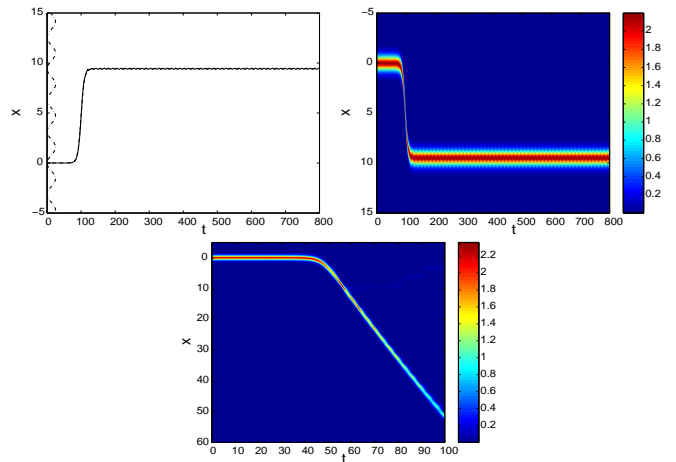


FIG. 4: (color online) The same as the previous figure, but with $\Omega = 0$ (i.e., in the absence of the magnetic trap). For $t_0 = 100$ and $\tau = 10$ (top panels) the soliton is delivered to its final location of $x_{\text{fin}} = 3\pi$. However, the same is not true for $t_0 = 50$ and $\tau = 5$ in the bottom panel, where the soliton fails to stop but rather continues its motion, losing more and more of its power through emission of radiation.

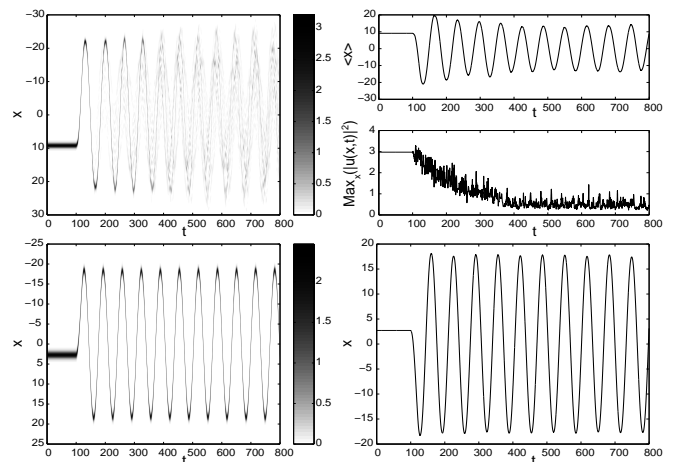


FIG. 5: Motion of the soliton induced by the linear ramp in Eq. (13) with $t_1 = 100$ and $t_2 = 120$. The top panel shows the case with strong radiation loss in a deep OL ($V_0 = 0.25$); notice apparent friction in the motion of the soliton's center of mass in the top right panel, and the corresponding loss of the soliton's norm in the panel below it. On the contrary, in the case of the shallow OL, with $V_0 = 0.07$ (the bottom panel), the moving soliton does not generate any visible radiation. In both cases, $\tau = 1$ was used.

with

$$\alpha(t) = 0.1 \times \frac{1}{2} \left[\tanh\left(\frac{t - t_1}{\tau}\right) - \tanh\left(\frac{t - t_2}{\tau}\right) \right]. \quad (13)$$

In Eq. (13), t_1 and t_2 are, respectively, the initial and final moment of time, between which the linear ramp is applied to accelerate the soliton to a finite propagation speed. We display two such numerical simulations in Fig. 5. The

first is performed in a deep OL, with $V_0 = 0.25$, taking initially the soliton in the third well ($t_1 = 100$ and $t_2 = 120$ were used). The second simulation was performed in a shallow OL, with $V_0 = 0.07$, the soliton being initially taken in the first well (the only one existing at such values of the parameters). The top panels clearly show that the emission of radiation leads to the gradual decay of the soliton's amplitude. On the contrary, when the OL is weaker (in the bottom panels), the soliton moves through it practically without radiation loss.

IV. CONCLUSION

We have examined a number of static and dynamic features of bright matter-wave (MW) solitons in the presence of the magnetic trap and optical lattice (OL). We used the perturbation theory to predict the existence and stability of the MW solitons trapped in the combined potential. A sequence of saddle-node bifurcations of the effective potential, which lead to consecutive disappearance of the higher-well solitonic bound states with the decrease of the OL strength was predicted, through the disappearance of the potential wells in the effective potential.

Having identified the stability characteristics of the dif-

ferent wells analytically, and verified it numerically, we then explored a possibility to use the OL as a tool to manipulate the soliton. We were able to stop the soliton at a prescribed location by turning on the OL, in an appropriate fashion. We have also found the adiabaticity condition necessary to secure the transfer of the soliton by a moving OL (with and without the magnetic trap). Finally, we have shown the absence of any visible emission of radiation from the soliton moving across a weak OL; however, the soliton loses a large fraction of its norm, moving through a stronger lattice.

Given the recent prediction of solitons and vortices in multi-dimensional OL potentials [4] (for recent experimental work on a similar topic in nonlinear optics, see Refs. [37, 38] and references therein), it would be of particular interest to implement similar dragging and manipulation of solitons in higher dimensions. The consideration of this case is currently in progress.

This work was partially supported by NSF-DMS-0204585, NSF-CAREER, and the Eppley Foundation for Research (PGK); the Israel Science Foundation grant No. 8006/03 (BAM); and the San Diego State University Foundation (RCG). PGK also gratefully acknowledges the hospitality of the Center for Nonlinear Studies of the Los Alamos National Laboratory. Work at Los Alamos is supported by the US DoE.

-
- [1] F. Dalfovo, S. Giorgini, L. P. Pitaevskii, and S. Stringari, *Rev. Mod. Phys.* **71**, 463 (1999); A. J. Leggett, *ibid.* **73**, 307 (2001); E.A. Cornell and C.E. Wieman, *ibid.* **74**, 875 (2002); W. Ketterle, *ibid.* **74**, 1131 (2002).
- [2] S. Burger, K. Bongs, S. Dettmer, W. Ertmer, K. Sengstock, A. Sanpera, G. V. Shlyapnikov, and M. Lewenstein, *Phys. Rev. Lett.* **83**, 5198 (1999); J. Denschlag, J. E. Simsarian, D. L. Feder, C. W. Clark, L. A. Collins, J. Cubizolles, L. Deng, E. W. Hagley, K. Helmerson, W. P. Reinhardt, S. L. Rolston, B. I. Schneider, and W. D. Phillips, *Science* **287**, 97 (2000); B. P. Anderson, P. C. Haljan, C. A. Regal, D. L. Feder, L. A. Collins, C. W. Clark, and E. A. Cornell, *Phys. Rev. Lett.* **86**, 2926 (2001).
- [3] K. E. Strecker, G. B. Partridge, A. G. Truscott, and R. G. Hulet, *Nature* **417**, 150 (2002); L. Khaykovich, F. Schreck, G. Ferrari, T. Bourdel, J. Cubizolles, L. D. Carr, Y. Castin, and C. Salomon, *Science* **296**, 1290 (2002);
- [4] B. B. Baizakov, V. V. Konotop, and M. Salerno, *J. Phys. B* **35**, 5105 (2002); E.A. Ostrovskaya and Yu.S. Kivshar, *Phys. Rev. Lett.* **90**, 160407 (2003).
- [5] B. Eiermann, Th. Anker, M. Albiez, M. Taglieber, P. Treutlein, K.-P. Marzlin, and M.K. Oberthaler, *Phys. Rev. Lett.* **92**, 230401 (2004).
- [6] B. B. Baizakov, B.A. Malomed, and M. Salerno, *Europhys. Lett.* **63**, 642 (2003).
- [7] B. B. Baizakov, B.A. Malomed, and M. Salerno, in: *Nonlinear Waves: Classical and Quantum Aspects*, ed. by F.Kh. Abdullaev and V.V. Konotop, p. 61 (Kluwer Academic Publishers: Dordrecht, 2004); *Multidimensional solitons in a low-dimensional periodic potential*, *Phys. Rev. A*, in press.
- [8] B.A. Anderson and M.A. Kasevich, *Science* **282**, 1686 (1998); M. Jona-Lasinio, O. Morsch, M. Cristiani, N. Malossi, J. H. Müller, E. Courtade, M. Anderlini, and E. Arimondo, *Phys. Rev. Lett.* **91**, 230406 (2003); V.V. Konotop, P.G. Kevrekidis, and M. Salerno, arXiv:cond-mat/0404608.
- [9] C. Orzel, A.K. Tuchman, M.L. Fenselau, M. Yasuda, and M.A. Kasevich, *Science* **291**, 2386 (2001).
- [10] O. Morsch, J.H. Muller, M. Cristiani, D. Ciampini, and E. Arimondo, *Phys. Rev. Lett.* **87**, 140402 (2001).
- [11] F.S. Cataliotti, S. Burger, C. Fort, P. Maddaloni, F. Minardi, A. Trombettoni, A. Smerzi, and M. Inguscio, *Science* **293**, 843 (2001).
- [12] M. Greiner, I. Bloch, O. Mandel, T.W. Hänsch, and T. Esslinger, *Phys. Rev. Lett.* **87**, 160405 (2001).
- [13] M. Greiner, O. Mandel, T. Esslinger, T.W. Hänsch, and I. Bloch, *Nature (London)* **415**, 39 (2002).
- [14] A.E. Leanhardt, A.P. Chikkatur, D. Kielpinski, Y. Shin, T.L. Gustavov, W. Ketterle, and D.E. Pritchard, *Phys. Rev. Lett.* **89**, 040401 (2002); H. Ott, J. Fortagh, S. Kraft, A. Gunther, D. Komma, and C. Zimmermann, *Phys. Rev. Lett.* **91**, 040402 (2003);
- [15] W. Hänsel, P. Hommelhoff, T.W. Hänsch, and J. Reichel, *Nature* **413**, 498 (2001); R. Folman and J. Schmiedmayer, *Nature* **413**, 466 (2001); J. Reichel, *Appl. Phys. B* **74**, 469 (2002); R. Folman, P. Krueger, J. Schmiedmayer, J. Denschlag and C. Henkel, *Adv. Atom. Mol. Opt. Phys.* **48**, 263 (2002).
- [16] Yu.S. Kivshar and G.P. Agrawal, *Optical Solitons: From Fibers to Photonic Crystals* (Academic Press, San Diego,

- 2003).
- [17] K. Mølmer, *New J. Phys.* **5**, 55 (2003).
- [18] D.I. Choi and Q. Niu, *Phys. Rev. Lett.* **82**, 2022 (1999).
- [19] A. Smerzi, A. Trombettoni, P.G. Kevrekidis, and A.R. Bishop, *Phys. Rev. Lett.* **89**, 170402 (2002); F.S. Cataliotti, L. Fallani, F. Ferlaino, C. Fort, P. Maddaloni, M. Inguscio, *New J. Phys.* **5**, 71 (2003).
- [20] P.G. Kevrekidis and D.J. Frantzeskakis, *Mod. Phys. Lett. B* **18**, 173 (2004).
- [21] V.A. Brazhnyi and V.V. Konotop, *Mod. Phys. Lett. B* **18**, 627 (2004).
- [22] V.M. Pérez-García, H. Michinel and H. Herrero, *Phys. Rev. A* **57**, 3837 (1998); for a more rigorous derivation of the 1D effective equation (in the case of repulsion, rather than attraction), see a paper by E.H. Lieb, R. Seiringer, and J. Yngvason, *Phys. Rev. Lett.* **91**, 150401 (2003).
- [23] Y.B. Band, I. Towers, and B.A. Malomed, *Phys. Rev. A* **67**, 023602 (2003).
- [24] L. Salasnich, A. Parola and L. Reatto, *Phys. Rev. A* **65**, 043614 (2002).
- [25] O. Morsch and E. Arimondo, in *Dynamics and Thermodynamics of Systems with Long-Range Interactions*, T. Dauxois, S. Ruffo, E. Arimondo and S. Wilkens (Eds.) (Springer, Berlin 2002), pp. 312–331.
- [26] Yu.S. Kivshar and B.A. Malomed, *Rev. Mod. Phys.* **61**, 763 (1989).
- [27] R. Scharf and A.R. Bishop, *Phys. Rev. E* **47**, 1375 (1993).
- [28] T. Kapitula, *Physica D* **156**, 186 (2001).
- [29] M. Grillakis, J. Shatah and W. Strauss, *J. Funct. Anal.* **74**, 160 (1987); *ibid.* **94**, 308 (1990).
- [30] T. Kapitula, P.G. Kevrekidis and B. Sandstede, *Physica D*, **195**, 263 (2004).
- [31] D.E. Pelinovsky, *Inertial law for spectral stability of solitary waves in coupled nonlinear Schrödinger equations*, preprint (2003).
- [32] Y.-J. Oh, *Comm. Math. Phys.* **121**, 11 (1989); *J. Diff. Eq.* **81**, 255 (1989).
- [33] W. Kohn, *Phys. Rev.* **123**, 1242 (1961); J.F. Dobson, *Phys. Rev. Lett.* **73**, 2244 (1994).
- [34] U. Al Khawaja, H.T.C. Stoof, R.G. Hulet, K.E. Strecker, and G.B. Partridge, *Phys. Rev. Lett.* **89**, 200404 (2002).
- [35] J.J. Garcia-Ripoll and V.M. Perez-Garcia, arXiv: ptt-sol/9904006.
- [36] H.E. Nistazakis, P.G. Kevrekidis, B.A. Malomed, D.J. Frantzeskakis, and A.R. Bishop, *Phys. Rev. E* **66**, 015601(R) (2002).
- [37] D.N. Neshev, T.J. Alexander, E.A. Ostrovskaya, Yu.S. Kivshar, H. Martin, I. Makasyuk, and Z. Chen, *Phys. Rev. Lett.* **92**, 123903 (2004).
- [38] J.W. Fleischer, G. Bartal, O. Cohen, O. Manela, M. Segev, J. Hudock, and D.N. Christodoulides, *Phys. Rev. Lett.* **92**, 123904 (2004).